PHILOSOPHICAL TRANSACTIONS OF THE ROYAL SOCIETY A MATHEMATICAL, PHYSICAL & ENGINEERING SCIENCES

Metamorphic Rocks of the 1985 Tibet Geotraverse, Lhasa to Golmud

N. B. W. Harris, T. J. B. Holland and A. G. Tindle

Phil. Trans. R. Soc. Lond. A 1988 **327**, 203-213
doi: 10.1098/rsta.1988.0126

Phil. Trans. R. Soc. Lond. A **327**, 203–213 (1988) [203]
Printed in Great Britain

Metamorphic rocks of the 1985 Tibet Geotraverse, Lhasa to Golmud

By N. B. W. Harris[1], T. J. B. Holland[2] and A. G. Tindle[1]

[1] *Department of Earth Sciences, The Open University, Walton Hall, Milton Keynes MK7 6AA, U.K.*
[2] *Department of Earth Sciences, University of Cambridge, Cambridge CB2 3EQ, U.K.*

Two examples of uplifted basement have been studied in the Lhasa Terrane of the Tibetan Plateau. The Nyainqentanglha orthogneisses are bounded by staurolite–garnet schists to the north which record prograde metamorphism at 5.0 ± 1.3 kbar, 610 ± 70 °C. Garnet–sillimanite xenoliths within the orthogneiss suggest that peak temperatures reached at least 700 ± 70 °C at 5.1 ± 2.5 kbar. These P/T fields reflect high T/low P metamorphism during Eocene subduction, and indicate that the syn-tectonic Nyainqentanglha orthogneiss was emplaced at depths greater than 10 km.

Sillimanite-bearing assemblages from the Amdo gneisses in the northern Lhasa Terrane provide evidence of crustal anatexis at temperatures > 680 °C. This event is poorly constrained in time but is probably Cambrian or earlier.

Within the Kunlun Terrane, biotite and garnet isograds north of the Xidatan Fault indicate an increase in metamorphic grade from north to south, reaching peak metamorphism at 470 ± 30 °C, 4.3 ± 1.5 kbar synchronous with the emplacement of the Triassic batholith. Regional metamorphism was followed by uplift of at least 2 km before emplacement of post-tectonic, early Jurassic granites.

1. Introduction

The Tibetan Plateau results from the collision of at least three continental fragments; the Lhasa, Qiangtang and Kunlun Terranes (Chang *et al.* 1986). The Zangbo Suture, which marks the site of ocean closure to the south of the Lhasa Terrane, also marks the boundary between metamorphic facies. South of the suture, high grade metamorphic basement is exposed with garnet-, kyanite- or sillimanite-bearing pelites defining a series of reverse metamorphic zones (Bordet *et al.* 1981; Burg *et al.* 1984). Metamorphic grade reaches a peak around the Main Central Thrust of the Himalayas, where assemblages indicate an eroded cover of at least 20 km. North of the Zangbo Suture in the southern Lhasa Terrane, assemblages in the sedimentary cover are indicative of low pressure greenschist metamorphism, and phases such as cordierite and andalusite are generally controlled by the thermal effects of granitoid emplacement (Burg *et al.* 1987). Throughout much of the Lhasa Terrane, cover rocks are generally unmetamorphosed except at the base of thrust sheets, as occurs east of Nagqu. However, in two regions, north of the Nyainqentanglha Mountains and south of Amdo (figure 1) uplifted blocks of basement have exposed deeper levels of the crust which provide medium-high grade metamorphic assemblages. No such basement is exposed in the Qiangtang Terrane along the line of the Geotraverse route. Further north in the Kunlun Terrane, low grade phyllonites are common in the region of the Xidatan Fault, and to the north of the fault biotite and garnet isograds have been located.

2. Techniques

All minerals were analysed on the wavelength dispersive electron microprobe at the Open University. Metamorphic conditions have been estimated by calculations based on extensions to the data-set of Holland & Powell (1985). These extensions involve addition of the phases almandine, annite and celadonite white mica, which have been made consistent with several experimental phase equilibria including Ferry & Spear (1978) and Bohlen *et al.* (1983). Celadonite data has been incorporated following Powell & Evans (1983). Activities for solid phase components in minerals were calculated by assuming ideal mixing on sites (phlogopite, clinochlore, annite), the Newton–Haselton (1981) formulation for garnet activities (pyrope, almandine, grossular), and the Price (1985) and Newton–Haselton (1981) activities for sanidine and anorthite; for muscovite and celadonite ideal mixing on site activities were used but a non-ideal Na–K contribution to the alkali ion site was introduced using the mixing parameters from Chatterjee & Flux (1986). The advantage of using the Holland & Powell (1985) data-set (including extensions described above) is that not only are the equilibria self-consistent but, more importantly, the uncertainties can be realistically assessed (see Powell & Holland, in press).

3. Metamorphism in the Lhasa Terrane

(*a*) *Carboniferous metasediments at Nagqu*

Ten kilometres east of Nagqu, Carboniferous phyllites are overthrust onto Cretaceous red beds (X40, figure 1). The phyllitic assemblages comprise sericite–chlorite–quartz–plagioclase–magnetite, and contain both a penetrative fabric (S_1) and crenulations of that fabric (S_2). Syn-D_2 euhedral chloritoid and andalusite overgrow S_1. The chloritoid (85% Fe, 12% Mg, 3% Mn) is a low-Mn phase, indicative of low-medium grade metamorphism. In the presence of andalusite, $T < 540$ °C, $P < 3$ kbar conditions are suggested (Hoschek 1967; Richardson 1968; Holdaway 1971) and the assemblage andalusite-quartz in the absence of pyrophyllite implies $T > 420$ °C (Kerrich 1968).

(*b*) *Metapelites from the Nyainqentanglha Range*

A 1 km wide band of staurolite-bearing phyllites is exposed within the metasedimentary sequence of carbonates and conglomerates in the northern section of the Nyainqentanglha Range. This is a distinctive horizon (X7, figure 1) containing large porphyroblasts of staurolite (1 cm), and locally andalusite (10 cm); it can be traced 15 km along strike to the south-west. The assemblage throughout this horizon is quartz–plagioclase–biotite–muscovite–staurolite–garnet–ilmenite. Staurolite forms syn-D_2 coarse porphyroblasts with rotated inclusion trails. Garnet grew somewhat earlier (late D_1) and is frequently included in staurolite. In one sample fibrolite, preserved as inclusions in plagioclase, coexists with coarse post-tectonic andalusite.

Further south in the Nyainqentanglha, schistose pelitic xenoliths within the granitic gneisses contain the assemblage quartz–plagioclase–muscovite–biotite–garnet–sillimanite (X12). Sillimanite is strongly aligned with biotite which defines the primary foliation (S_1), but muscovite appears to be post-tectonic and retrogressive. Since the fabric of the Nyainqentanglha orthogneiss implies syn-D_1 emplacement, the P/T conditions of the schist provides valuable evidence for the emplacement conditions of the granite gneiss.

The location of these assemblages in the Thompson A-F-M projection (figure 2) clearly show

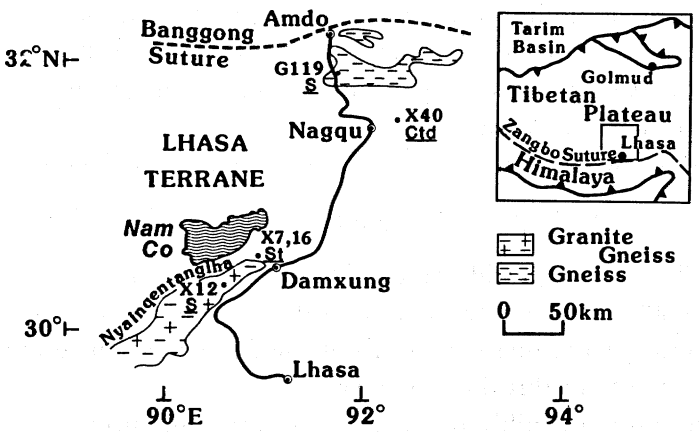

FIGURE 1. Sketch location map showing distribution of metamorphic samples from Lhasa Terrane. Index minerals given by St = staurolite, S = sillimanite, Ctd = chloritoid.

that staurolite from the phyllites lies within the garnet–sillimanite–biotite three phase triangle, indicating its instability within the P/T conditions of the sillimanite-schists.

This relationship can be represented by the equilibrium

$$\text{Staurolite} + \text{Quartz} = \text{Garnet} + \text{Sillimanite} + H_2O \qquad (1)$$

the staurolite in the phyllites forming at lower temperatures than the garnet and sillimanite in the schist.

To determine peak metamorphic conditions of the phyllite, temperatures can be constrained by the equilibrium

$$\text{Fe-Biotite} + \text{Pyrope} = \text{Almandine} + \text{Mg-Biotite}. \qquad (2)$$

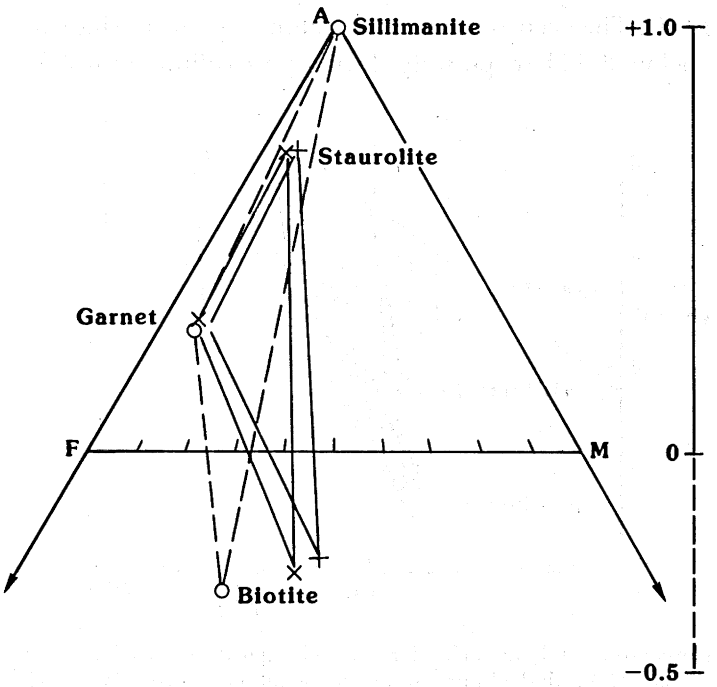

FIGURE 2. A((Al$_2$O$_3$–3K$_2$O)/(Al$_2$O$_3$–3K$_2$O+FeO+MgO)), F(FeO), M(MgO) diagram projected through muscovite (Thompson projection) for Nyainqentanglha samples. + = X7, O = X12, X = X16.

Analyses of non-contiguous biotite–garnet pairs indicate that the garnet grew during increasing temperatures since the rims give temperatures about 40 °C above these determined from the cores (tables 1 & 2). Average peak temperatures lie in the range 610±70 °C, based on the experimental study of Ferry & Spear (1978).

A second equilibrium which can be used as a thermometer is given by

$$\text{Alkali feldspar} + \text{Paragonite} = \text{Albite} + \text{Muscovite}. \quad (3)$$

This has been calibrated over a wide range of P/T conditions by Green & Usdansky (1986). Temperatures of ~ 600 °C have been determined from the staurolite-bearing phyllites, in agreement with biotite–garnet thermometry, but the free energy uncertainty in the reaction implies a large uncertainty in this thermometer.

To determine pressures of equilibration, the water-free equilibrium

$$\text{Pyrope} + \text{Grossular} + \text{Muscovite} = \text{Anorthite} + \text{Phlogopite} \quad (4)$$

has been calibrated using the self-consistent data set of Holland & Powell (1985). The addition of annite and almandine to the data-set provides the Fe end-member reaction

$$\text{Almandine} + \text{Grossular} + \text{Muscovite} = \text{Anorthite} + \text{Annite}. \quad (5)$$

At 610 °C, these give pressures of 4.6±1.6 kbar and 4.9±1.2 kbar respectively. Reactions 2, 4 and 5 computed from garnet core compositions intersect at 5.0 kbar, 630 °C. The absence of sillimanite, except as occasional fibrolite inclusions in plagioclase, indicates that reaction (1) has not occurred. Based on the experimental data of Dutrow & Holdaway (1986), $a_{H_2O} > 0.6$ is required for staurolite + quartz to be stable without sillimanite at about 630 °C (figure 3).

Application of these equilibria to the observed assemblages indicates that they formed under conditions of increasing temperature and lie on a prograde P-T-t loop which passes through 5±1 kbar, 610±30 °C. The occurrence of post-tectonic andalusite indicates that metamorphic growth continued below 3.5 kbar, possibly during post-collisional uplift.

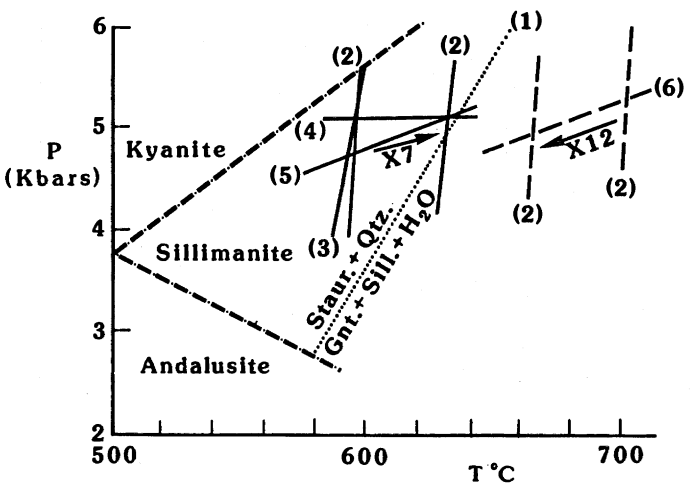

FIGURE 3. Pressure–temperature stability fields for staurolite–garnet–muscovite phyllite (X7, solid lines) and sillimanite-garnet schist (X12, dashed lines) from Nyainqentanglha Mts. Arrows give change of temperature during garnet growth. Numbers in parentheses refer to equilibria in text. (Equilibrium 1 computed for $a_{H_2O} = 0.6$).

Application of biotite–garnet equilibria to the sillimanite schists suggests that garnet grew during decreasing temperatures from 700–660 °C. Temperatures of ~ 600 °C determined from plagioclase–muscovite thermometry (3) confirm the retrograde nature of muscovite. Pressures in the absence of primary muscovite, can be estimated from the equilibrium

$$\text{Grossular} = \text{Anorthite} + \text{Sillimanite} + \text{Quartz}. \qquad (6)$$

Using the data-set of Holland & Powell (1985) pressures at 700 °C are 5.1 ± 2.5 kbar (the large uncertainty resulting from low grossular activity in garnet and poorly constrained γ_{an}). Conditions of D_1 metamorphism are given by 700 ± 70 °C, 5.1 ± 2.5 kbar, which places a minimum depth of emplacement for the Nyainqentanglha granite of around 10 km. Since the granite gneisses have been dated by zircon studies at about 50 Ma (Xu *et al.* 1985), it can be concluded that the penetrative fabric of S_1 occurred during a compressive regime at an active continental margin. The high geothermal gradient implied by the sillimanite schists is consistent with such a setting. Subsequent collision resulted in uplift recorded by post-tectonic growth of andalusite in some phyllites.

(*c*) *The Amdo gneisses*

Ten kilometres south of Amdo, an uplifted block (50×50 km^2) of granitic and amphibolite gneiss is exposed bounded by vertical faults to the north and east, and thrust south over Permo–Triassic limestone. Zircon ages of 530 Ma, and model Nd ages of 1240 Ma bracket the time of emplacement of these gneisses. (Harris, Xu, Lewis, Hawkesworth & Zhang, this volume). Schlieren of pelitic paragneiss within the basement contain the assemblage quartz–plagioclase–perthite–biotite–muscovite–sillimanite. The sillimanite forms prograde epitaxial sheaths within or around biotite crystals which define the penetrative schistosity, D_1. The gneisses contain granitic augen (probably anatectic leucosomes), enveloped by restite phases, biotite and sillimanite.

Muscovite appears to be post-D_1 formed by solid state reaction between sillimanite and alkali feldspar. This is confirmed by muscovite–plagioclase equilibria ~ 570 °C (reaction 3), considerably lower than granite melting temperatures. Since muscovite was not apparently stable on the solidus, maximum pressures and temperatures can be obtained from the intersection between the granite melting curve and the equilibrium

$$\text{Muscovite} + \text{Quartz} = \text{Alkali feldspar} + \text{Sillimanite} + H_2O. \qquad (7)$$

Applying microprobe analyses to the internally consistent data-set of Holland & Powell (1985), this intersection for $a_{H_2O} = 1$ is located at $T = 650 \pm 15$ °C, $P = 4.0 \pm 0.5$ kbar (table 3). Unfortunately conditions of $a_{H_2O} < 1$ will significantly increase the pressure of this intersection and consequently the assemblage does not provide a useful pressure constraint. A minimum temperature of 570 °C is obtained from the muscovite–plagioclase thermometer. It is assumed muscovite formed from reaction (7), $a_{H_2O} = 0.5$ for reactions (3) and (7) to intersect in the sillimanite stability field (figure 4), although the large uncertainty in the muscovite–plagioclase thermometer poorly constrains this intersection. Melting under such conditions requires $T > 680$ °C (Kerrich 1972) which places a probable minimum peak temperature constraint on anatexis in the gneisses.

Two-feldspar thermometry records a rather approximate temperature of about 530 °C (using the calibration of Price 1985), reflecting retrograde perthite exsolution in the alkali feldspar.

PHILOSOPHICAL TRANSACTIONS OF THE ROYAL SOCIETY A MATHEMATICAL, PHYSICAL & ENGINEERING SCIENCES

PHILOSOPHICAL TRANSACTIONS OF THE ROYAL SOCIETY A MATHEMATICAL, PHYSICAL & ENGINEERING SCIENCES

TABLE 1. MICROPROBE ANALYSES FROM GARNET (G) – STAUROLITE (S) – BIOTITE (B) – MUSCOVITE (M) – PLAGIOCLASE (P) – QUARTZ ASSEMBLAGE (X7, NYAINQENTANGLHA)

	G1 core	G1 rim		S1	S2		B1	B2	M1	M2		P1	P2
SiO_2	39.93	37.91	SiO_2	28.33	28.76	SiO_2	34.93	34.95	44.79	45.55	SiO_2	59.67	60.40
TiO_2	0.07	0.05	TiO_2	0.59	0.68	TiO_2	1.65	1.54	0.69	0.45	Al_2O_3	25.82	25.42
Al_2O_3	20.74	21.29	Al_2O_3	55.10	54.97	Al_2O_3	18.99	19.28	33.70	35.31	FeO	0.06	0.14
FeO	30.69	31.74	FeO	12.85	13.04	FeO	19.75	19.82	2.73	1.30	CaO	7.56	7.04
MnO	4.85	4.53	MnO	0.28	0.31	MnO	0.11	0.11	0.02	0.02	Na_2O	7.33	7.49
MgO	2.56	2.94	MgO	1.35	1.27	MgO	9.74	9.70	1.00	0.50	K_2O	0.06	0.19
CaO	2.46	2.61	Na_2O	0.02	0.02	CaO	0.04	0.01	0.22	0.01	Total	100.50	100.68
Total	101.30	101.07	ZnO	0.25	0.29	Na_2O	0.16	0.25	1.18	1.17			
			Total	98.77	99.34	K_2O	8.92	9.57	9.64	9.89			
						Total	94.29	95.23	93.97	94.20			
	Atoms to 12(O)		Atoms to 44(O)			Atoms to 22(O)					Atoms to 8(O)		
Si	3.13	3.01	Si	7.75	7.82	Si	5.38	5.35	6.10	6.13	Si	2.65	2.67
Al	1.92	1.99	Al	17.77	17.63	Al	3.44	3.47	5.41	5.60	Al	1.35	1.33
Fe	2.01	2.11	Ti	0.12	0.14	Ti	0.19	0.18	0.07	0.05	Ca	0.36	0.33
Mn	0.32	0.30	Fe	2.94	2.97	Fe	2.54	2.54	0.31	0.15	Na	0.63	0.64
Mg	0.30	0.35	Mn	0.06	0.07	Mn	0.01	0.01	0.00	0.00	K	0.00	0.01
Ca	0.21	0.22	Mg	0.55	0.52	Mg	2.23	2.21	0.20	0.10			
			Zn	0.05	0.06	Na	0.05	0.07	0.31	0.30			
						K	1.75	1.87	1.67	1.70			

All iron calculated as FeO.

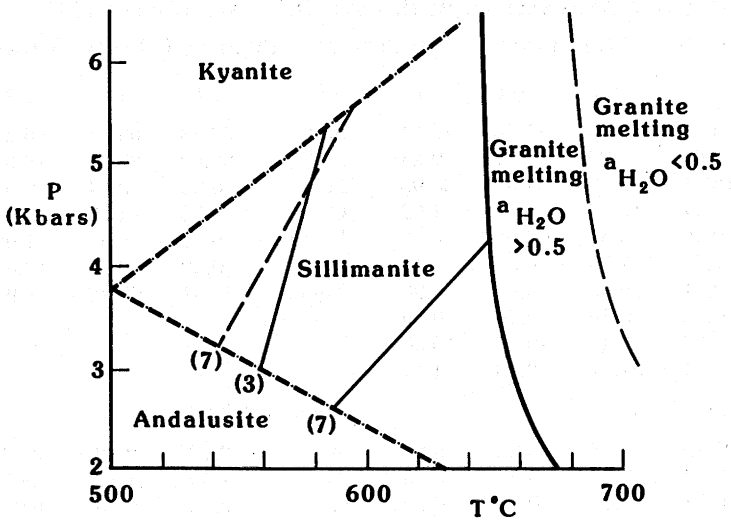

FIGURE 4. Pressure–temperature stability field for sample G119 (sillimanite gneiss) from Amdo basement. Dashed lines indicate $a_{H_2O} = 0.5$; Solid lines $a_{H_2O} = 1$.

TABLE 2. MICROPROBE ANALYSES FROM GARNET (G) – BIOTITE (B) – MUSCOVITE (M) – PLAGIOCLASE (P) – SILLIMANITE – QUARTZ ASSEMBLAGE (X12, NYAINQENTANGLHA)

	G1 core	G1 rim		B1	B2	M1	M2		P1	P2
SiO_2	37.16	37.15	SiO_2	34.54	34.31	44.93	45.07	SiO_2	62.56	62.51
TiO_2	0.02	0.03	TiO_2	2.86	2.78	0.71	0.75	Al_2O_3	22.64	22.91
Al_2O_3	20.92	21.01	Al_2O_3	18.92	19.04	34.67	34.29	FeO	0.03	0.04
FeO	31.39	31.08	FeO	23.30	22.60	1.81	2.07	CaO	4.25	4.50
MnO	8.75	9.06	MnO	0.38	0.31	0.03	0.05	Na_2O	9.36	9.22
MgO	1.87	1.77	MgO	5.99	6.05	0.48	0.54	K_2O	0.17	0.14
CaO	0.87	0.96	CaO	0.01	0.03	0.01	0.00	Total	99.01	99.32
Total	100.98	101.06	Na_2O	0.26	0.19	0.74	0.80			
			K_2O	9.37	9.39	10.27	10.36			
			Total	95.63	94.70	93.65	93.93			
Atoms to 12(O)			Atoms to 22(O)					Atoms to 8(O)		
Si	3.00	3.00	Si	5.36	5.36	6.11	6.13	Si	2.80	2.79
Al	1.99	2.00	Al	3.46	3.51	5.56	5.49	Al	1.19	1.20
Fe	2.12	2.10	Ti	0.33	0.33	0.07	0.08	Ca	0.20	0.21
Mn	0.60	0.62	Fe	3.02	2.95	0.21	0.24	Na	0.81	0.80
Mg	0.23	0.21	Mn	0.05	0.04	0.00	0.00	K	0.01	0.01
Ca	0.08	0.08	Mg	1.38	1.41	0.10	0.11			
			Na	0.08	0.04	0.19	0.21			
			K	1.85	1.87	1.78	1.80			

All iron calculated as FeO.

Tonalitic orthogneisses from the Amdo basement record a Jurassic age for sphene growth and a Cambrian age for zircon growth (Xu *et al.* 1985). The most likely interpretation of the limited data available is that the sphene age records only a low grade event, and that the high grade anatexis observed in the gneisses records an earlier, possibly Cambian event.

PHILOSOPHICAL TRANSACTIONS OF THE ROYAL SOCIETY A MATHEMATICAL, PHYSICAL & ENGINEERING SCIENCES

TABLE 3. MICROPROBE ANALYSES FROM BIOTITE (B) – MUSCOVITE (M) – PLAGIOCLASE (P) – PERTHITE (K) – SILLIMANITE – QUARTZ ASSEMBLAGE (G119B, AMDO BASEMENT)

	B1	B2	M1	M2		P1	P2	K1	K2
SiO_2	35.22	35.49	45.78	46.14	SiO_2	62.53	63.18	65.24	64.85
TiO_2	2.98	1.86	0.17	0.24	Al_2O_3	22.69	22.28	18.01	18.16
Al_2O_3	18.81	19.66	34.52	35.03	FeO	0.06	0.04	0.03	0.03
FeO	21.27	19.89	1.11	1.02	CaO	4.72	4.21	0.04	0.01
MnO	0.40	0.32	0.02	0.03	Na_2O	9.11	9.35	1.98	1.29
MgO	7.43	7.79	0.55	0.49	K_2O	0.20	0.16	13.64	14.70
CaO	0.01	0.03	0.01	0.00	Total	99.31	99.22	98.94	99.04
Na_2O	0.20	0.20	0.70	0.69					
K_2O	9.52	9.47	10.37	10.50					
Total	95.84	94.71	93.23	94.14					
Atoms to 22(O)					Atoms to 8(O)				
Si	5.39	5.45	6.22	6.20	Si	2.79	2.82	3.02	3.01
Al	3.40	3.56	5.53	5.55	Al	1.19	1.17	0.98	0.99
Ti	0.34	0.22	0.02	0.02	Ca	0.23	0.20	0.00	0.00
Fe	2.72	2.55	0.13	0.12	Na	0.79	0.80	0.18	0.12
Mn	0.05	0.04	0.00	0.00	K	0.01	0.01	0.80	0.87
Mg	1.70	1.78	0.11	0.10					
Na	0.06	0.06	0.19	0.18					
K	1.86	1.86	1.80	1.80					

All iron calculated as FeO.

4. METAMORPHISM IN THE KUNLUN TERRANE

The development of metamorphic minerals in the supracrustal rocks of the Kunlun terrane is restricted to phyllitic and phyllonitic outcrops within 15 km of the Xidatan Fault. Approaching the fault from the north, pelites contain the greenschist assemblage chlorite–quartz ± sericite ± biotite ± magnetite (G200C). Within 10 km of the fault, a garnet-in isograd strikes north-east (figure 5). This results in the assemblage biotite–chlorite–muscovite–garnet–quartz ± ilmenite (X63). The garnet is skeletal and deformed by the penetrative foliation (D_1). The appearance of garnet within this zone is sporadic and composition controlled. Sediments adjacent to post-tectonic granites show thermal metamorphism superimposed on the regional facies. Fe-rich post-kinematic cordierite is developed along the eastern contact of the Xiaonanchuan granite (G213D) in a biotite–muscovite–cordierite–quartz ± tourmaline hornfels in which chlorite has been replaced by post-kinematic biotite. The post-S_2 fabric and high Fe content (42% Mg end-member) of the cordierite argue for its contact metamorphic origin. West of the Xidatan granite post-D_1 andalusite (pseudomorphed by sericite) occurs in a biotite–chlorite–muscovite–quartz phyllite (X68C). The andalusite pseudomorphs predate the east–west fabric recorded in the granite parallel to the Xidatan fault. It is likely that andalusite growth and granite emplacement were concurrent, and both deformed by subsequent movement along the Xidatan fault zone. South of the fault, neither garnet nor contact phenomena have been recorded and pelitic phyllonites contain the assemblage chlorite–sericite–quartz similar to those observed 15 km north of the fault.

The garnet-bearing assemblage (X63) provides biotite–garnet pairs for thermometry (equilibrium 2), but the high Mn content of garnet results in a large uncertainty on the

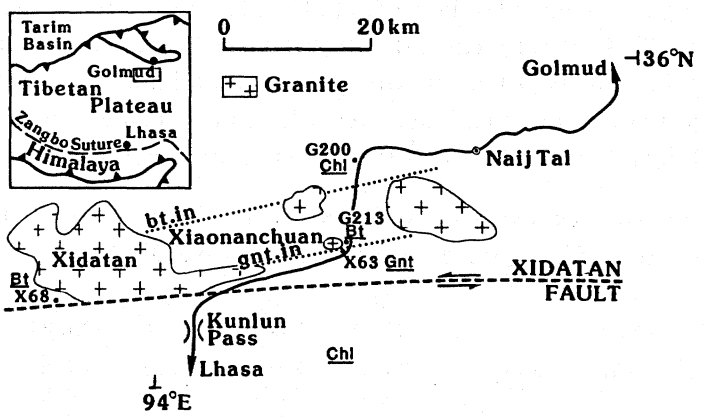

FIGURE 5. Sketch location map showing distribution of metamorphic samples from Kunlun Terrane. Index minerals given by Chl (chlorite), Bt (biotite), Gnt (garnet).

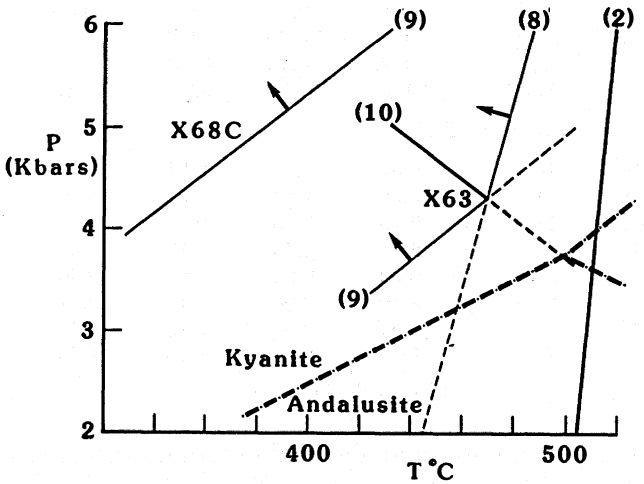

FIGURE 6. Pressure–temperature stability field for samples X63 (garnet–biotite–muscovite–chlorite) and X68C (biotite–muscovite–chlorite) from Kunlun Mts., north of Xidatan Fault. Numbers in parentheses refer to equilibria in text. Arrows indicate limiting constraints provided by solid phase equilibria, assuming $a_{H_2O} = 1$.

calculated temperature 500–520 °C (table 4). A dehydration reaction with steep slope in P/T space is provided by the equilibrium

$$\text{Celadonite} + \text{Clinochlore} = \text{Pyrope} + \text{Phlogopite} + \text{Quartz} + H_2O. \quad (8)$$

Using the data-set of Holland & Powell (1985), extended to include celadonite, a maximum temperature of 470 ± 30 °C is obtained at 5 kbar for garnet-bearing samples.

Minimum pressures (or maximum temperatures) for Kunlun samples north of the fault can be computed for muscovite–biotite–chlorite assemblages through the equilibrium

$$\text{Celadonite} + \text{Clinochlore} = \text{Muscovite} + \text{Phlogopite} + \text{Quartz} + H_2O \quad (9)$$

as calibrated by Powell & Evans (1983). For samples containing the additional phase garnet the vapour-absent equilibrium

$$\text{Celadonite} + \text{Pyrope} = \text{Muscovite} + \text{Phlogopite} + \text{Quartz} \quad (10)$$

may be written. Using the extended data-set of Holland & Powell (1985) reactions (9) and (10) provide pressures at 470 °C of 4.3 ± 1.5 and 4.3 ± 2.1 kbar respectively (figure 6). This defines a model invariant point (for fixed Fe/Mg ratio and a_{H_2O}) at 4.3 kbar, 470 °C for sample X63. Sample X68C (a garnet-absent assemblage) records somewhat lower peak temperatures but with a large uncertainty (340 ± 70 °C at 4.0 kbar based on reaction 9).

TABLE 4. MICROPROBE ANALYSES FROM GARNET (G) – BIOTITE (B) – MUSCOVITE (M) – CHLORITE (C) – QUARTZ ASSEMBLAGES (X63, X68C, KUNLUN)

	G1 (X63)	G2 (X63)		B1 (X63)	B1 (X68C)	M1 (X63)	M1 (X68C)	C1 (X63)	C1 (X68C)
SiO_2	41.01	39.73	SiO_2	36.05	32.08	42.02	47.09	24.88	24.89
TiO_2	0.23	0.14	TiO_2	0.26	0.66	0.24	0.39	0.09	0.09
Al_2O_3	20.08	20.14	Al_2O_3	18.16	22.22	36.19	33.71	21.99	23.41
FeO	20.04	20.20	FeO	18.83	18.81	1.58	2.51	24.07	22.25
MnO	12.38	13.22	MnO	0.26	0.32	0.02	0.03	0.46	0.46
MgO	1.18	1.17	MgO	10.11	13.06	0.83	0.88	14.75	16.19
CaO	6.13	6.33	CaO	0.01	0.01	0.03	0.09	0.03	0.01
Total	101.05	100.93	Na_2O	0.14	0.09	0.72	1.37	0.02	0.02
			K_2O	9.52	4.13	10.19	9.12	0.01	0.01
			Total	94.71	91.38	97.82	95.19	86.30	87.33
	Atoms to 12(O)		Atoms to 22(O)					Atoms to 28(O)	
Si	3.20	3.14	Si	5.51	4.95	6.21	6.28	5.30	5.18
Al	1.85	1.88	Al	3.28	4.04	5.51	5.30	5.53	5.75
Ti	0.01	0.01	Ti	0.18	0.08	0.02	0.04	0.01	0.01
Fe	1.31	1.33	Fe	2.41	2.43	0.17	0.28	4.29	3.87
Mn	0.82	0.88	Mn	0.03	0.04	0.00	0.00	0.08	0.08
Mg	0.14	0.14	Mg	2.30	3.00	0.16	0.17	4.69	5.02
Ca	0.51	0.54	Na	0.04	0.03	0.18	0.35	0.01	0.01
			K	1.86	0.81	1.68	1.55	0.00	0.00

All iron calculated as FeO.

The post-D_1 andalusite in the thermal aureole of the Xidatan granite, and the cordierite hornfels of the Xiaonanchuan granite both suggest emplacement at $P < 3.5$ kbar. This implies that at least 2 km uplift occurred between regional greenschist metamorphism observed in the country rock and intrusion of the Kunlun granites at depths no greater than 10 km. The syntectonic granite emplacement ages of 240–260 Ma (Harris, Xu, Lewis, Hawkesworth & Zhang, this volume) indicate a Triassic age for regional greenschist metamorphism.

5. CONCLUSIONS

Throughout the Lhasa and Qiangtang Terranes, supracrustal rocks are generally unmetamorphosed although temperatures of $490 + 70$ °C are recorded at the base of some thrust sheets. Basement gneisses exposed south of Amdo comprise the oldest known rocks from the terranes and granitic leucosomes within sillimanite-bearing pelites indicate temperatures in excess of 680 °C. A second uplifted region exposed north of the Eocene Nyainqentanglha orthogneisses is characterized by staurolite-andalusite pelites which equilibrated under prograde conditions at 5.0 ± 1.3 kbar, 610 ± 70 °C. Xenoliths within the orthogneisses provide garnet–sillimanite assemblages which have equilibrated at 700 ± 70 °C, 5.1 ± 2.5 kbar. The implied steep geothermal gradient probably resulted from thermal convection associated with voluminous granite emplacement at an active continental margin. More than 10 km of cover is indicated during emplacement of the gneisses.

PHILOSOPHICAL TRANSACTIONS OF THE ROYAL SOCIETY A MATHEMATICAL, PHYSICAL & ENGINEERING SCIENCES

Pelites from the Kunlun Terrane are characterized by low grade chlorite-sericite assemblages. However north of the Xidatan Fault both biotite-in and garnet-in isograds have been identified from a regional metamorphic event which is synchronous with the Triassic emplacement of the syn-tectonic Kunlun batholith. Maximum metamorphic grade has been determined from garnet-bearing metasediments at 4.3 ± 1.5 kbar, 470 ± 30 °C. Post-kinematic cordierite and andalusite from post-tectonic granite aureoles suggest > 2 km of uplift occurred between regional metamorphism and post-collision granite emplacement.

The authors gratefully acknowledge Marilyn Leggett for typing the manuscript and John Taylor for drafting the diagrams.

References

Bohlen, S. R., Wall, V. J. & Boettcher, A. L. 1983 Experimental investigations and geological applications of equilibria in the system FeO–TiO_2–Al_2O_3–SiO_2–H_2O. *Am. Mineral.* **68**, 1049–1058.

Bordet, P., Colchen, M. & Le Fort, P. 1981 The geodynamic evolution of the Himalaya – Ten years of research in Central Nepal Himalaya and some other regions. *Geodynamic Ser.* **3**, *Am. geophys. Un.*, pp. 149–168.

Burg, J.-P., Giraud, M., Chen, G. M. & Li, G. C. 1984 Himalayan metamorphism and deformations in the North Himalayan Belt (southern Tibet, China). *Earth planet. Sci. Lett.* **63**, 391–400.

Burg, J.-P., Leyreloup, A., Girardeau, J. & Chen Guo-Ming 1987 Structure and metamorphism of a tectonically thickened continental crust: the Yalu-Tsangpo suture zone (Tibet). *Phil. Trans. R. Soc. Lond.* A **321**, 67–86.

Chang Chengfa *et al.* 1986 Preliminary conclusions of the Royal Society and Academia Sinica 1985 geotraverse of Tibet. *Nature Lond.* **323**, 501–507.

Chatterjee, N. D. & Flux, S. 1986 Thermodynamic mixing properties of muscovite–paragonite crystalline solutions at high temperatures and pressures, and their geological applications. *J. Petrol.* **27**, 677–693.

Dutrow, B. L. & Holdaway, M. J. 1986 Upper thermal stability of Staurolite + Quartz at medium pressures: a reinvestigation. *Terra Cogn.* **6**, 24 (abstr.).

Ferry, J. H. & Spear, F. S. 1978 Experimental calibration of the partitioning of Fe and Mg between biotite and garnet. *Contr. Mineral. Petrol.* **66**, 113–117.

Green, N. L. & Usdansky, S. I. 1986 Toward a practical plagioclase–muscovite thermometer. *Am. Mineral.* **71**, 1109–1117.

Hoschek, G. 1967 Untersuchungen zum stabilitats bereich von chloritoid und staurolith. *Contr. Mineral. Petrol.* **14**, 123–162.

Holdaway, M. J. 1971 Stability of andalusite and the aluminium silicate phase diagram. *Amer. J. Sci.* **271**, 97–131.

Holland, T. J. B. & Powell, R. 1985 An internally consistent thermodynamic data-set with uncertainties and correlations: 2: Data and results. *J. metamorph. Geol.* **3**, 343–370.

Kerrich, D. M. 1968 Experiments on the upper stability limit of pyrophyllite at 1.8 Kbars and 3.9 Kbars water pressure. *Am. J. Sci.* **266**, 204–214.

Kerrich, D. M. 1972 Experimental determination of muscovite + quartz stability with $P_{H_2O} < P_{total}$. *Am. J. Sci.* **272**, 946–958.

Newton, R. C. & Haselton, H. T. 1981 Thermodynamics of the Garnet–Plagioclase–Al_2SiO_5–Quartz geobarometer. In *Thermodynamics of minerals and melts* (ed. R. C. Newton, A. Narrotsky and B. J. Wood), pp. 129–145. New York: Springer-Verlag.

Powell, R. & Evans, J. 1983 A new geobarometer for the assemblage biotite–muscovite–chlorite–quartz. *J. metamorph. Geol.* **1**, 331–336.

Powell, R. & Holland, T. J. B. 1987 An internally consistent dataset with uncertainties and correlations. 3: application methods, worked examples and a computer program. *J. Mm. Geol.* (In press.)

Price, J. G. 1985 Ideal site mixing in solid solutions with an application to two-feldspar geothermometry. *Am. Mineral.* **70**, 696–701.

Richardson, S. W. 1968 Staurolite stability in a part of the system Fe–Al–Si–O–H. *J. Petrol.* **9**, 467–488.

Xu Ronghua, Scharer, U. & Allègre, C. J. 1985 Magmatism and metamorphism in the Lhasa Block (Tibet): a geochronological study. *J. Geol.* **93**, 41–57.

PHILOSOPHICAL TRANSACTIONS OF THE ROYAL SOCIETY A MATHEMATICAL, PHYSICAL & ENGINEERING SCIENCES